JOURNAL OF MATERIALS SCIENCE 31 (1996) 2885–2892

Effect of chromium content on remarkably rapid nitriding in austenitic Fe–Ni–Cr alloys

K. GEMMA, T. TAHARA, M. KAWAKAMI
Department of Materials Science, Tokai University, 1117 Kitakaname, Hiratsuka 259-12, Japan

Remarkably rapid nitriding which is independent of diffusion theory based on the thermal activation process, was observed during nitriding of austenitic Fe–Ni–Cr steels containing 16 and 19 mass % chromium. Increase of the chromium content in the alloys yielded increasing thickness of the nitrided layer, i.e. the internal nitriding theory did not hold in the nitriding. No rapid nitriding was observed in steels containing less than 13 mass % chromium. Hence the limiting concentration of chromium for the rapid nitriding will lie between 13 and 16 mass % chromium. A solution to the problem of abnormalities arising during nitriding of practical austenitic stainless steels which have been investigated since 1972, has been presented experimentally by nitriding various chromium-containing steels. Based on the experimental results, the origin of the rapid nitriding is discussed in connection with the free-energy function of Cr_2N and CrN to temperature. In particular, a plateau of nitrogen concentration measured in the nitrided layers leads to the conclusion that a forced nitrogen diffusion in the layer resulted in the rapid nitriding.

1. Introduction

During the nitriding of austenitic stainless steels (for example types 304 and 316 steels), abnormal phenomena have been found: first a remarkably rapid nitriding in the temperature range 723–873 K, and second a sudden decrease of the rate of nitriding above 873 K [1–7]. The cause of the rapid nitriding and the sudden decrease in the steels have been discussed from various points of view: first the precipitation of ferrite was studied based on the iron–nickel phase diagram in the nitrided layer [1], second, the formation of microcracks in the nitrided layer was investigated during nitriding [2], and recently a cyclic mechanism of the formation and decomposition of a nitrogen-supersaturated solid solution, γ_{SN} phase, in the nitrided layer have been pointed out during nitriding [4–7]. The layer of γ_{SN} phase formed has been reported as a nitride-free phase [8] with fcc or fct structure [9], and also reported to contain over 40 at % nitrogen in the layer [10]. We have examined the remarkably rapid nitriding in type 304 steel to originate from the austenitic chemical composition of the steel itself [6]. Based on the results, a high manganese–high chromium austenitic steel was nitrided, and similar abnormalities to those observed in the austenitic stainless steels were found in the steel [11]. Thus the chromium in the steels seem to play the role of the main element for the abnormalities. From this point of view, the effect of the chromium content on the rapid nitriding was investigated in various austenitic Fe–Ni–Cr steels.

2. Experimental procedure

2.1. Preparation of specimens

Electrolytic iron and chromium plate and nickel tablet were prepared. Table 1 shows the chemical analysis of these metals. A sum of about 50 g of these metal chips were weighed by chemical balance to prepare the specimens containing 7–19 mass % chromium as shown in Table 2. The mixture of these chips was melted three times by means of electric arc melting method in a copper crucible cooled under argon atmosphere, and a button-like ingot was obtained in the crucible. The ingot was annealed at 1423 K for 86.4 ks in hydrogen atmosphere using a laboratory electric furnace and quenched into the sodium hydroxide aqueous solution of 10 mass %. The ingot was then cold rolled into sheet of 1.0 mm thick with process annealing in hydrogen atmosphere. The sheet was annealed at 1423 K for 3.6 ks and quenched again in the same manner (solution treatment). The crystal structure of the solution treated specimens was examined by X-ray diffractometry to note if the phase of the alloys become into full austenite or not. Figure 1 shows XRD patterns obtained from the solution treated specimens. The profiles A and B in the figure are the patterns of the alloy 7 Cr and 19 Cr shown in Table 2, respectively. In both profiles, austenite peaks are detected strongly with very weak ferrite peaks. From these diffraction angles, the lattice parameters of austenite in the steels are calculated as 0.359 nm, respectively. Other alloys containing intermediate chromium content among the 7–19% Cr, shown in

0022–2461

TABLE I Chemical analysis (mass %) of the raw materials used for preparation of the specimens

Materials	C	S	P	Si	Mn	Cu	N	O	Al	Ni	Cr	Fe
Electrolytic Fe	0.0029	0.0036	< 0.004	< 0.005	< 0.005	< 0.004	0.0016	0.047				Bal
Electrolytic Cr	0.004	0.027	0.002	0.001		0.0001	0.029	0.43	0.001		99.35	0.14
Nickel pellet	< 0.01	0.0003				0.0001				> 99.97		

TABLE II Composition of alloys prepared and used (mass %)

Alloy	Fe	Ni	Cr
7Cr	73	20	7
10Cr	72	18	10
13Cr	71	16	13
16Cr	73	11	16
19Cr	70	11	19

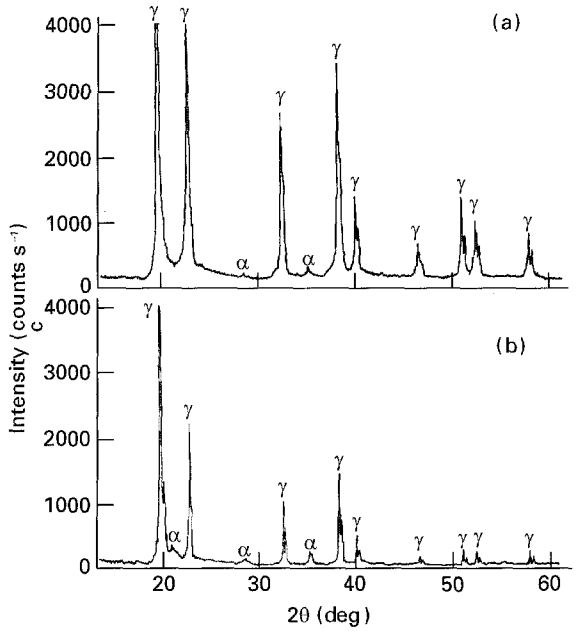

Figure 1 XRD patterns obtained from the solution-treated alloys prepared, for Alloys (a) 7Cr and (b) 19Cr shown in Table II.

Table 2, also show similar diffraction patterns. Pieces of 15 mm × 20 mm in dimensions were cut down from the sheet, for nitriding specimens. Preliminary polishing and degreasing for the surface of the specimens before nitriding has been described in previous papers [4–7]. After the preliminary treatment, the specimens were immediately supplied for nitriding.

2.2. Nitriding

Specimens were nitrided at a temperature range 723–853 K for 7.2–32.4 ks in an ammonia gas atmosphere. The method of the nitriding has been described in previous papers [4–7]. After nitriding, the nitrided surface of the specimens was analysed by X-ray diffractometry using a rotating molybdenum target and applied 50 kV of tube voltage with 70 mA by the step scanning method. Optical microscopic observation and line scanning analysis by EPMA were carried out for the nitrided layer.

3. Experimental results

3.1. Optical microstructure

Fig. 2 shows optical microphotographs of specimens containing 7–19% Cr nitrided at 853 K for 32.4 ks. The nitrided layers formed in the alloy 7Cr, 10Cr and 13Cr were grown to approximately 80 μm thick. On the other hand, the layers formed in the alloy 16Cr and 19Cr were grown to approximately 125 μm and 130 μm thick, respectively. These layers are clearly thicker than that formed in the alloy 7–13Cr. Thus it is first found that the rapid nitriding in the austenitic Fe–Ni–Cr is taking place in the alloys containing over 16 mass % Cr. Furthermore, the morphology of the nitrided layer changed with the Cr content in the steels, as shown in Fig. 2. In particular, the alloy 7Cr is interesting, very coarse precipitates grow from a grain boundary to the core of the grain, and also from the front of the nitrided proceeding layer to the inner growing layer and precipitating in the layer. In the alloy 10Cr, similar precipitates are also observed in the nitrided layer, however, the layer is corroded rather darkly more than that formed in the alloy 7Cr. The corrosiveness in the nitrided layer seems to increase with increasing chromium content up to the alloy 13Cr. In the alloy 13Cr, the nitrided layer is completely covered by inter- and transgranular precipitates. Similarities in the nitrided layers formed in the alloys 7Cr to 13Cr are indistinct at the front of the layers. In contrast with these alloys, the alloys 16Cr and 19Cr exhibit clear edge-like fronts of the layers, and individual precipitates in the layers can no longer be observed optically. Moreover, these layers are clearly thickened more than the layers formed in alloys containing less than 13 mass % Cr. Thus optical microscopic observation indicates that there is a limiting chromium content in the austenitic Fe–Ni–Cr steels at which the remarkably rapid nitriding can take place. Because this rapidity is considered to be naturally related to the rapid nitrogen diffusion in the nitrided layer, this problem will be discussed later in connection with the concentration gradient of nitrogen in the layer measured by EPMA. The nitrided structure formed in the low temperature range, such a 723 K nitrided for 32.4 ks, is shown in Fig. 3. Fig. 3a shows the nitrided layer formed in the 10Cr alloy in which no rapid nitriding has taken place, and Fig. 3b shows that in the alloy 19Cr the rapid nitriding has definitely taken place. The morphology of the nitrided layer of the 10Cr alloy, as seen in Fig. 3a, shows a bright and white nitrided layer, 15 μm thick, formed with very fine and stringy precipitates crossing each other under the surface of the alloy. This layer seems to be hard etched in contrast with the alloy matrix which was clearly etched. In the 19Cr alloy, too, the

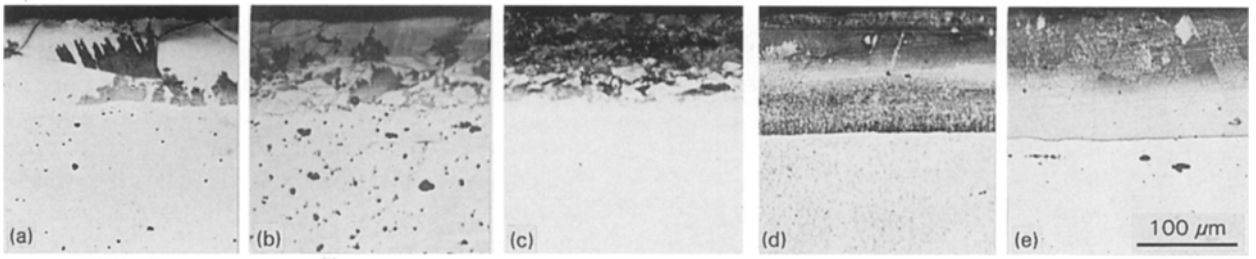

Figure 2 Optical micrographs of various chromium-containing alloys nitrided at 853 K for 32.4 ks. (a) Alloy 7Cr, (b) alloy 10Cr, (c) alloy 13Cr, (d) alloy 13Cr and (e) alloy 19Cr.

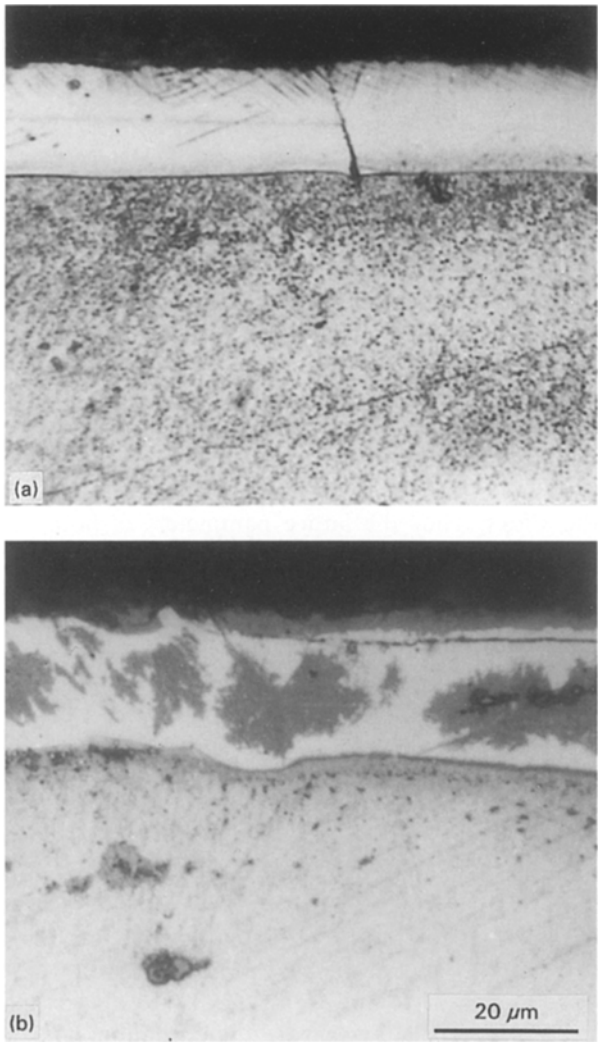

Figure 3 Optical micrographs of the nitrided layers formed in alloys (a) 10Cr and (b) 19Cr nitrided at 723 K for 32.4 ks.

hard-etched phase was also observed in the 25 μm thick nitrided layer; however, a very coarse and dark phase occupies almost half the space of the layer. Furthermore, the dark phase was also formed just below the surface. Thus it is suggested that both the formation of the hard-etched phase and precipitation in the phase must relate to the rapid nitriding. In ion nitriding of type 316 stainless steel at 623 K, similar hard-etched nitrided layers have been reported as an extreme nitrogen supersaturated f c c structure with an ε phase with its habit on the (1 1 1) plane of the lattice [10]. A temperature of 623 K is low enough to ensure no rapid nitriding takes place [4, 5]. On the contrary, at 723 K rapid nitriding is certain to occur [1, 2, 4, 5], and the hard-etched phase was formed at the 723 K in both the alloys 10Cr and 19Cr, as shown in Fig. 3. As has been reported, the hard-etched layer was formed stably by long-term nitriding, such as 218 ks at 673 K [8], and the rapid nitriding began above ~ 700 K [4, 5]. Therefore, the hard-etched layers formed at 723 K shown in Fig. 3 will be metastable, that is, the metastable hard-etched phase can be formed when the austenitic Fe–Ni–Cr alloys are nitrided in the temperature range in which the rapid nitriding has taken place.

3.2. Chromium content versus growth of nitrided layer

Chromium content versus growth of the nitrided layer, ξ, in the alloys 7Cr to 19Cr nitrided in the temperature range 723–853 K for 32.4 ks is shown in Fig. 4. Clearly the nitrided layers formed in the alloys 16Cr and 19Cr were thicker than those formed in other alloys containing less than 13 mass % Cr at all temperatures. In particular, in the alloys 16Cr and 19Cr, the thickness of the nitrided layers were increased with increasing chromium content. However, the layers formed in other alloys were observed to be the same thickness, regardless of the chromium content. Although these nitrided layers were observed to be the same thickness optically, the nitrogen migration depth in the layers were slightly decreased with increasing chromium content, as shown later by EPMA analysis. Thus different kinetics must be considered in the nitriding of the austenitic Fe–Ni–Cr steels in the chromium content range over 16 mass % and under 13 mass %, that is, a rigid chromium concentration for the change of the nitriding mechanism will lie between the alloys. Fig. 5 shows time dependence of the rapid nitriding in the alloys 7Cr to 19Cr at 723 K. Below 14.4 ks, all specimens exhibit no effects of the rapid nitriding. On prolonging the time for 32.4 ks, the alloys 16Cr and 19Cr were clearly nitrided rapidly. Thus, at a not-so-high temperature of 723 K, rapid nitriding was observed to begin after an incubation period.

3.3. Nitrogen concentration distribution

Fig. 6 shows line-scanning profiles for the nitrogen in the nitrided layers formed in the alloys 7Cr to 19Cr

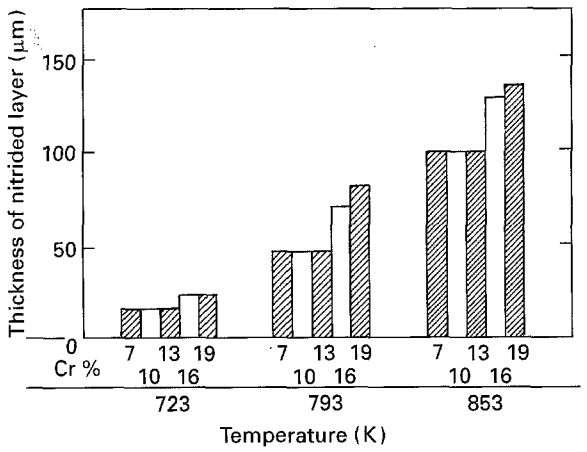

Figure 4 Effect of chromium content on the growth of the nitrided layer in various chromium-containing alloys nitrided at 723–853 K for 32.4 ks.

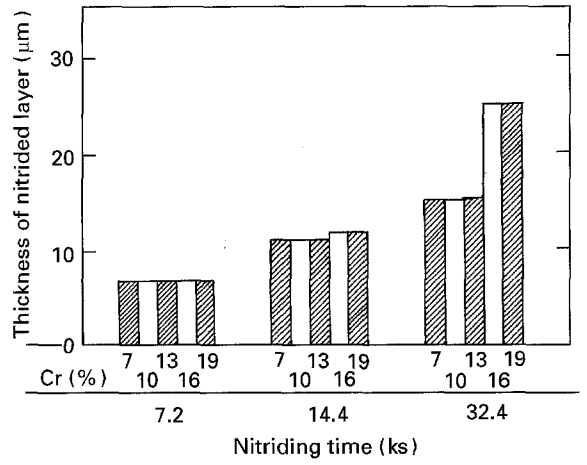

Figure 5 Effect of nitriding time on the growth of the nitrided layer in various chromium-containing alloys nitrided at 723 K for 7.2–32.4 ks.

nitrided at 853 K for 32.4 ks. Profiles of (a–e) in Fig. 6 refer to specimens (a–e) as shown in Fig. 2, respectively. It is shown that the nitrogen concentration in the nitrided layer is proportional to the chromium content of the alloys. In particular, the surface nitrogen concentrations are heightened in the alloys 16Cr and 19Cr rapidly nitrided. The migration depth of the nitrogen in the alloys 7Cr, 10Cr and 13Cr are evaluated to be approximately 95, 95 and 90 μm, respectively. In the alloys 16Cr and 19Cr, it is evaluated to be approximately 125 and 135 μm, respectively. Thus the nitrogen migration depth was decreased slightly with increasing chromium content up to the alloy 13Cr. On the contrary, this tendency is reversed in alloys 16Cr and 19Cr. Another characteristic of these nitride layers is the nitrogen concentration gap between the nitrided layer and the alloy phase. The gap in the alloys 16Cr and 19Cr in which rapid nitriding takes place was shown to broaden suddenly. On the other hand, the alloys 7Cr and 10Cr, in which no rapid nitriding takes place, showed a loose gap, or rather, an ordinary nitrogen concentration gradient. The gap was also observed in the alloy 13Cr; however, mostly a thin nitrided layer was formed in the alloy described above. The result suggests that near 13 mass % chromium is the critical concentration at which rapid nitriding may or may not take place. Furthermore, the most noteworthy characteristic in the nitrogen concentration gradient is a plateau which appears in the gradient near the front of the nitrided layers formed in the alloys 16Cr and 19Cr. As the plateau was not formed in the layer of nitrided alloys 7Cr to 13Cr, it is evident that the plateau resulted in the accelerated diffusion of nitrogen taking place in the layers, and that the acceleration must be derived from the higher nitrogen concentration area formed under the surface of the alloys, see the patterns (d) and (e) in Fig. 6. Thus a forced diffusion of the nitrogen atoms during the nitriding of the austenitic stainless steels can be explained from the viewpoint of the effect of chromium content in the steels.

3.4. X-ray analysis

Fig. 7 shows XRD patterns obtained from the surface of the specimens nitrided at 853 K for 32.4 ks. Profiles (a–e) refer to specimens (a–e) in Fig. 2, namely, profile (a) was obtained from nitrided specimen (a). The profiles in Fig. 7 show very similar diffraction patterns, and a CrN-like phase (◆) and a γ'-Fe_4N-like phase (marked γ'_N) were observed. All diffraction peaks on the profiles were observed to be shifted slightly to the low-angle side with increasing chromium content in the alloys. Thus the lattice parameters of both fcc phases formed in these specimens were changed with the chromium content. The relationship between the lattice parameters and the chromium content is summarized in Table III. With respect to the CrN like phase, the lattice parameter of the phase was increased with increasing the chromium content over 13% Cr, however both the alloy 7Cr and 10Cr showed the same value of approximately 0.4103 nm compared with the value of 0.4140 nm referred to in the CrN phase [12]. On the other hand, the lattice constant of the γ'-Fe_4N-like phase was in agreement with that of γ'-Fe_4N phase of 0.3795 nm [13] over 13 mass % chromium alloys. The lattice parameters measured from the profiles of alloys 7Cr and 10Cr, however, were calculated to be 0.3774 and 0.3781 nm, respectively. These results, regardless of chromium content in the alloys, seem to indicate that both CrN and γ'-Fe_4N phases were formed at the surface of the nitrided layers. But the disappearance of diffraction lines of the (1 1 0) plane of γ'-Fe_4N in the XRD-patterns of the alloys 16Cr and 19Cr, and the appearance of the plane, albeit very weak, in the patterns of the alloys 7Cr to 13Cr, suggests the formation of an austenite with nitrogen (nitrogen austenite). Fig. 2a and b show the nitrogen austenite formation, because localized precipitations are observed in the nitrided matrix. The nitrided matrix is observed to be clearly different from that of the 10Cr alloy nitrided at 723 K as shown in Fig. 3a. Therefore, it is considered that these matrices consist of the nitrogen auEstenite. Now, on low-temperature nitriding at 723 K for 32.4 ks, the alloys 10Cr and 19Cr gave XRD-profiles such as are shown in Fig. 8; profiles (a) and (b) in the

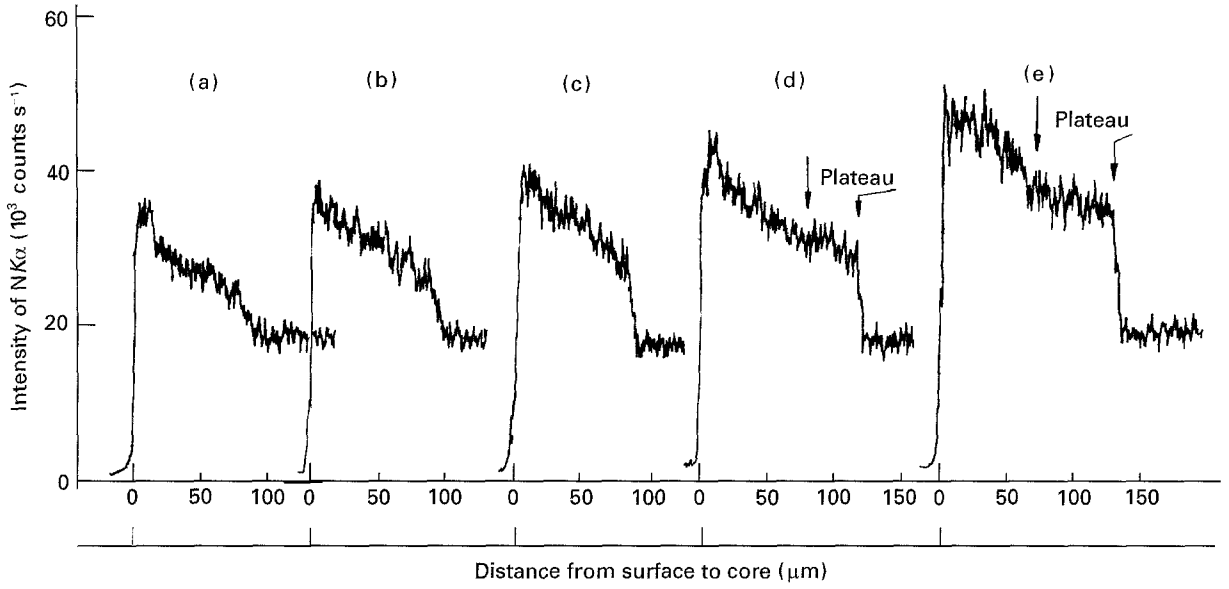

Figure 6 Nitrogen concentration distribution in the nitrided layers formed in various chromium-containing alloys nitrided at 853 K for 32.4 ks. (a) Alloy 7Cr, (b) alloy 10Cr, (c) alloy 13Cr, (d) alloy 13Cr and (e) alloy 19Cr.

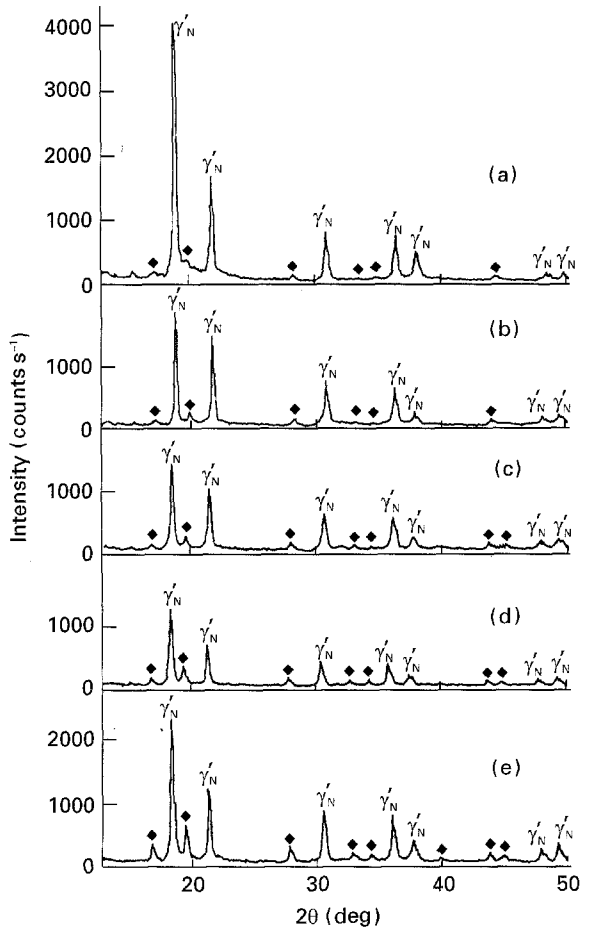

Figure 7 XRD patterns obtained from various chromium-containing alloys nitrided at 853 K for 32.4 ks. (a) Alloy 7Cr, (b) alloy 10Cr, (c) alloy 13Cr, (d) alloy 13Cr and (e) alloy 19Cr. (γ'_N) γ'-Fe N or nitrogen austenite, (◆) CrN-like phase.

figure were obtained from specimens (a) and (b) shown in Fig. 3, respectively. Both the profiles show a similar pattern in appearance of an fcc type phase and a CrN-like phase with broadened peaks. Because the nitrided layers are relatively thin, as shown in Fig. 3,

TABLE III Diffraction peak position, 2θ, and lattice parameter, a_0, of CrN-like and γ'-Fe_4N-like phase formed in various chromium containing alloys nitrided at 853 K for 32.4 ks

Nitrided alloys	CrN like phase[a]		γ'-Fe_4N like phase[b]	
	2θ (2 2 0) (deg)	a_0 (nm)	2θ (4 0 0) (deg)	a_0 (nm)
7Cr	28.3	0.4103	44.3	0.3774
10Cr	28.3	0.4103	44.2	0.3781
13Cr	28.0	0.4146	43.8	0.3795
16Cr	27.9	0.4160	43.8	0.3795
19Cr	27.8	0.4175	43.8	0.3795

[a] a_0 of CrN = 0.4140 nm [12].
[b] a_0 of γ'-Fe_4N = 0.3795 nm [13].

the diffractions of austenite from the base alloy appear on the high-angle side of the profiles. As shown in Fig. 3a, only a few very fine precipitates are observed in the nitrided layer. Therefore, XRD measurements will give mainly information on the matrix of the layer with that of the precipitate in the XRD profiles. Based on this viewpoint, the fcc-type phase is determined to be the matrix of the layer and a value of approximately 0.3871 nm for the lattice parameter is given. This value is larger than that of 0.3795 nm in γ'-Fe_4N phase [12]. Also in profile (b) in Fig. 8, the lattice parameter of the fcc phase is calculated to be approximately 0.3929 nm. Thus it is considered that the nitrided layer formed at 723 K consists of a nitrogen-supersaturated solid solution with the CrN-like phase. With respect to the CrN-like phase in the profiles, the phase was clearly detected on profiles (a) and (b) in Fig. 8, in spite of a only few precipitates being observed. The diffraction angle, 2θ, of the (1 1 1) plane of the CrN-like phase on profile (a) (alloy 10Cr) was measured at 19.3° shifted slightly from the 19.7° of that plane of the CrN phase [13]. On the other hand, as shown in profile (b) (alloy 19Cr), the diffraction angles of the phase are in good agreement with that of the CrN phase referred to

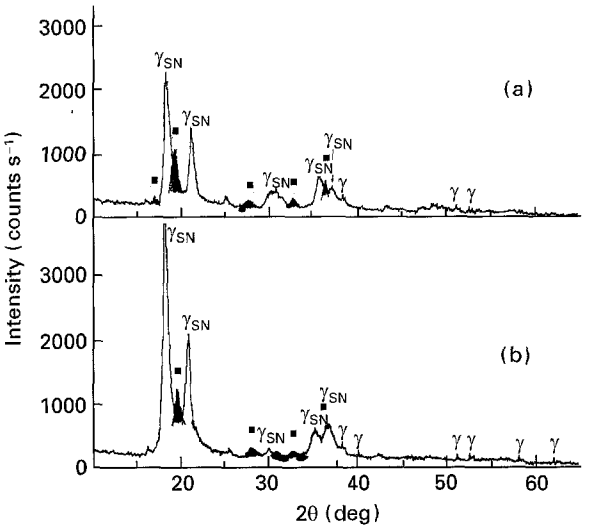

Figure 8 XRD patterns obtained from alloys 10Cr and 19Cr nitrided at 723 K for 32.4 ks; profiles (a) and (b) refer to Fig. 5a and b. γ_{SN} is the nitrogen supersaturated austenitic phase, γ is the austenite. (■) CrN.

above. Thus the phase noted here as the CrN-like phase is determined to be a distorted CrN. As a result, the nitrogen-supersaturated nitrided layer with distorted CrN phase was formed in both alloys of low (10 mass %) and high (19 mass %) chromium content at 723 K.

4. Discussion

The rates of nitriding of steels containing a nitride-former element (for example, chromium), have been discussed based on internal nitriding theory [2, 14, 15] as analogy to the internal oxidation theory [16, 17]. The nitriding theory shows that the rates of nitriding, and also growth of the nitrided layer, are inversely proportional to the chromium concentration in the steels. Mittemeijer [15] investigated the nitriding of ferritic steels containing 1.88 and 3.61 mass % Cr based on the formula

$$\xi^2 = 2([N]^s/[Cr])D_\alpha t \quad (1)$$

where ξ is the nitriding depth, $[N]^s$ is the nitrogen concentration at the surface of steels during nitriding, [Cr] is the chromium content in the steel, D_α is the diffusion constant of nitrogen in ferrite at the nitriding temperature, and t is the nitriding time. Billon and Hendry [2] used a similar formula for the nitriding of type 316 austenitic stainless steel which contained approximately 18 mass % Cr:

$$\xi^2 = (52/7)r^{-1}([N]^s/[Cr])D_\gamma t \quad (2)$$

where r is the ratio of nitrogen to chromium in the nitride formed, D_γ is the diffusion constant of nitrogen in austenite. These investigators concluded that the internal nitriding theory was valid in each steel. Kindlimann and Ansell [18] also concluded that the theory can be adapted to nitriding of austenitic Fe–Cr–Ni–Ti alloy. Thus all investigations on the nitriding of the steels containing chromium validated the theory. Contrary to these conclusions, the results in the present work indicate that the internal nitriding theory does not apply to the nitriding of the austenitic Fe–Ni–Cr steels. Because it has been reported to be adapted at high temperatures such as 1073 K [2], the theory may be applied to a normal diffusion mechanism, such as thermal activation processes. However, the abnormalities in the nitriding of austenitic stainless steels have remained an unsolved problem since 1972 [1]. Accordingly many investigators have investigated the abnormalities, and several models have been presented as explanations [1–3]. Because commercial alloys were used as specimens, such as types 304 and 316 steel, and no effect of chromium content was noted, the true reason for the abnormalities cannot be found from these models. Indeed, the nitrided layer formed in alloys 16Cr and 19Cr grew very much thicker than that formed in other alloys as shown in Fig. 2, and a characteristic precipitation was clearly observed in the layers, not at the front of the layer. When nitrides are formed at the front, the internal nitriding theory, in analogy to the internal oxidation theory, can be discussed. Therefore, the precipitation in the nitrided layer as shown in Fig. 3b during nitriding must influence the nitrogen diffusion in the layer. When the nitrogen-supersaturated nitrided layer, such as the γ_{SN} phase, as shown in the XRD profile b in Fig. 8 in decomposed into precipitates, there was an exothermic change of enthalpy. If free nitrogen atoms were co-precipitated in the layer, part of the enthalpy will be dissipated by the diffusion of the nitrogen atoms and the rest will be dissipated by heat conduction. An actual diffusion process is essentially a non-linear and non-equilibrium phenomenon; however, the theory for interstitial diffusion processes, such as nitriding (carburizing), has been discussed based on the assumption that the chemical potential of nitrogen (carbon) equilibrates at the interface between gas and metal, that is, between adsorbed nitrogen on the metal and dissolved nitrogen in the metal. In general, in diffusion processes, dissolved atoms behave as an atom flux from the surface to the core of a metal depending on the chemical potential gradient, and any chemical reactions are essentially avoided in the diffusion path [19]. Thus it is considered that the remarkably rapid nitriding is caused by an acceleration of nitrogen diffusion in the nitrided layers. Therefore, the problem consequent upon the rapid nitriding must be solved from a novel theory, such as the theory of the thermodynamics for non-linear and non-equilibrium phenomena [20] and [21]. In the historical background of the nitriding of steels, metallurgists have considered the technique to be too practical for engineering in industry. Consequently, neither physicists nor physical chemists have noticed this important phenomenon of rapid nitriding in the austenitic stainless steels, and the phenomenon has been shelved as an abnormality in the surface heat-treatment problems. It has now been proved that the effect of chromium content on the rapid nitriding of the austenitic Fe–Ni–Cr steels is as shown in Figs 2 and 6, i.e. a limiting concentration of chromium is shown to be needed in the steels in which the rapid nitriding is taking place. In addition, the rapid nitriding took

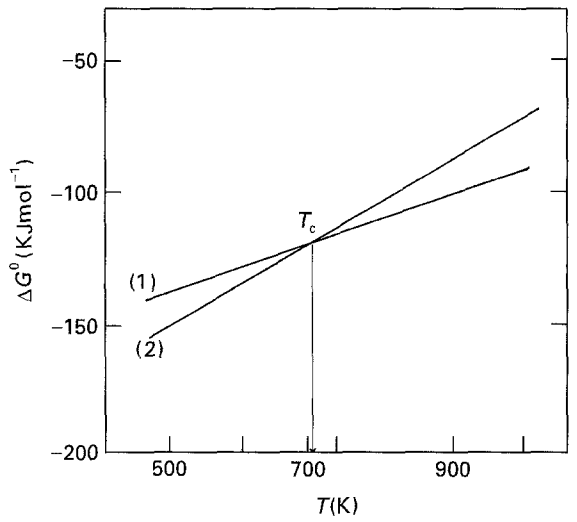

Figure 9 T–ΔG^0 diagram for standard free energy of formation of Cr_2N and CrN; T_C is the thermodynamic critical point for the nitrides. (1) $4Cr + N_2 = 2Cr_2N$, (2) $2Cr + N_2 = 2CrN$.

place above approximately 700 K [3, 4]. This temperature is in close agreement with the temperature at the intersection of free energy of Cr_2N and CrN on the T–ΔG° diagram as shown schematically in Fig. 9. Physical chemists are well accustomed in dealing with the phase transformation of pure substances based on such diagrams for chemical potential versus temperature [22]. A metastable state near the transformation point can also be seen on the diagrams. The reaction rate with a diffusion near the thermodynamic critical point mentioned above has attracted physicists [23, 24], because the chemical potentials between reactant and product approach zero at the equilibrium point, and therefore the diffusibility of atoms is extremely restricted. This principle gives an interesting consideration to the kinetics of nitriding below the temperature of the intersection of free energy of chromium nitrides. It is clearly observed that the nitrogen-supersaturated nitrided layer with no precipitates is formed in that temperature range [4, 5, 7, 8, 11], and the dissolved nitrogen in the layer will fluctuate between a tendency to form Cr_2N and CrN near or below the intersecting temperature. Theories of isothermal phase. transformation with precipitates in supersaturated alloys seem to be firmly established; however, the kinetics consist in the following restriction; the transformation takes place at the interface of the precipitate and the alloy matrix, and the chemical potential of the solute atom in the matrix gradually diminishes, together with the degree of precipitation. Contrary to the kinetics, the rapid nitriding at 723 K clearly showed both characteristics, i.e. the precipitation in the nitrided layer and the growth of the layer by diffusion control, simultaneously. If the intersection of the free energy function of chromium nitrides to temperature is related to the rapid nitriding, the abnormalities in the austenitic stainless steels can be treated scientifically, and detailed investigations based on a new standpoint are expected. As the thermodynamic critical point of the chromium nitrides exists at a convenient temperature, such as 700 K, this novel phenomenon was fortunately found while investigating surface heat-treatment engineering. As shown by the results here and in previous articles [3, 4], the rapid nitriding in the austenitic Fe–Ni–Cr steels and stainless steels takes place due to the following factors.

1. Chromium concentration dependence; the rapid nitriding definitely takes place in the alloy containing over 16 mass % Cr.

2. Critical temperature dependence: the rapid nitriding begins at approximately 700 K, in agreement with the intersection of the free energy function of chromium nitrides to temperature.

Factor 1 suggests that the supersaturation of nitrogen in the nitrided layer relates to the affinity of chromium to nitrogen as that of aluminium to nitrogen in iron pointed out by Darken [25], and that the degree of the supersaturation is proportional to the concentration of the chromium. Factor 2 suggests that the kinetics of the nitriding is changed at the intersection, and that the nitrogen-supersaturated phase (γ_{SN} phase) which is formed stably below 700 K [7–10] is formed metastably above the intersecting temperature. Thus the decomposition of the metastable γ_{SN} phase probably yields the rapid nitriding when the nitrogen concentration in the phase was over the limit of the degree of supersaturation, and then the decomposed γ_{SN} phase must be reformed immediately by neighbouring supersaturated nitrogen atoms supplied continuously by the decomposition of ammonia. During the time before the nitrogen concentration reaches the limit in the metastable phase, rapid nitriding will therefore be incubating, as shown in Fig. 5. Finally, the plateau in the nitrogen concentration gradient in the nitrided layers must be discussed, because a plateau concentration distribution in a cemented layer in alloys is generally formed by a surface reaction-controlling mechanism, and such a plateau should hold as a constant concentration from the surface to the front of the layer [19], while the plateaus formed in alloys 16Cr and 19Cr, as shown in Fig. 6, lay under the higher nitrogen concentrated layer formed under the nitrided surface. Depending on the interstitial atomic diffusion theory, such a nitrogen concentration gradient with the plateau cannot be considered. However, this theory seems to be applicable to the nitriding in low-chromium alloys of alloys 7Cr and 10Cr from the nitrogen concentration gradient, as shown in Fig. 6. Thus, the theory does not hold in such high-chromium alloys, but does in low-chromium alloys. Hence, the plateaus have resulted from the rising nitrogen concentration gradient caused by a forced and rapid diffusion of nitrogen in the nitrided layers. As mentioned previously, the cyclic mechanism of the formation and decomposition of the γ_{SN} phase which formed in the nitrided layer, has been presented as a model to explain the forced nitrogen diffusion [5–7]. The incubation of the onset of rapid nitriding was also shown and noted previously, based on the degree of supersaturation of nitrogen in connection with the chromium content in the alloys. It is concluded from the results that the driving force of the rapid nitrogen diffusion probably acted in the area of heightened concentration of nitrogen under the nitrided surface, shown in

the line-scanning profiles (d) and (e) in Fig. 6, and that the plateau in the nitrogen concentration gradient was formed as evidence. Since the development of EPMA analysis, measurement of the concentration distribution of elements in nitrided layers has become easy and common; however, no investigators have focused on the plateau as an important novel phenomenon.

5. Conclusions

To obtain an understanding of the abnormalities in the nitriding of austenitic stainless steels, particularly the remarkably rapid nitriding in the steels, austenitic Fe–Ni–Cr alloys containing 7–19 mass % Cr were nitrided in the range 723–853 K for 7.2–32.4 ks. Optical microscopy, X-ray diffractometry and EPMA analysis were made for observation of the nitrided layers formed. The following conclusions were drawn.

1. The remarkably rapid nitriding took place in alloys containing 16–19 mass % Cr in the temperature range 723–853 K; however, this has hardly been observed in other alloys containing less than 13 mass % Cr in same temperature range.

2. An incubation in the beginning of the rapid nitriding was observed at 723 K. After a duration of 32.4 ks, the rapid nitriding finally began in the alloys.

3. In optical microscopic observations for both alloys containing 10 and 19 mass % Cr, a hard-etched layer with a precipitate was observed. The layer was determined as the phase with an f c c lattice larger than γ'-Fe_4N lattice by X-ray diffractometry, and the precipitate was analysed as a distorted CrN phase.

4. The lattice parameters of the f c c phase formed in various alloys were changed depending on the chromium content in the alloys; the parameters in rapidly nitrided specimens were larger than that of γ'-Fe_4N; however, the parameters in specimens not rapidly nitrided were less than that of γ'-Fe_4N.

5. The nitrogen concentration just below the surface of the specimens increased with increasing chromium content in the alloys, and a plateau in the nitrogen concentration gradient was observed in the remarkably rapidly nitrided specimens containing 16 and 19 mass % Cr.

As a final point, it should be noted that the abnormalities in the nitriding of the austenitic stainless steels are real phenomena which lie outside the theory of a diffusion-controlling mechanism, so that the internal nitriding theory cannot be applied to the rapid nitriding, and the plateau of nitrogen concentration gradient formed in the nitrided layers is evidence of a forced nitrogen diffusion which yielded the remarkably rapid nitriding.

Acknowledgements

The authors thank Professor K. Tachikawa, Faculty of Engineering, Tokai University, for help in preparing specimens, and Mr Y. Miyamoto, Superior Technician, Faculty of Engineering, Tokai University, for the EPMA technique, and Y. Nishi, Department of Materials Science, and graduate students in his laboratory, for the X-ray techniques.

References

1. J.-P. LEBRUN, H. MICHEL and M. GANTOIS, *Mém. Sci. Rev. Métall.* **69** (1972) 727.
2. B. BILLON and A. HENDRY, *Surf. Eng.* **1** (1985) 125.
3. S. KIYO-OKA and T. HOMMA, *NETSU SHORI* **14** (1974) 33.
4. K. GEMMA and M. KAWAKAMI, *J. Jpn. Inst. Metals* **52** (1988) 701.
5. *Idem, High Temp. Mater. Proc.* **8** (1989) 205.
6. K. GEMMA, M. KAWAKAMI, H. UEDA and C. MIHARA, *J. Mater. Sci.* **27** (1992) 3461.
7. K. GEMMA, M. KAWAKAMI, H. UEDA, N. TOKUHARA, A. KANAYAMA and H. KASAHARA, in "Heat and Surface '92, The 8th International Congress on Heat Treatment of Materials", Kyoto, Japan, Nov. 17–20, 1992, edited by I. Tamura (Japan Technical Information Service, Tokyo) p. 381.
8. Z. L. ZHANG and T. BELL, *Surf. Eng.* **1** (1985) 131.
9. N. YASUMASU and K. KAMACHI, *J. Jpn. Inst. Metals* **50** (1986) 362.
10. S-P. HANNULA, P. NENONEN and J. MOLARIUS, in "High nitrogen steels HNS 88", Proceedings of the international conference, Lille France, May 18–20, 1988, edited by J. Fost and A. Hendry (The Institute of Metals, London) p. 266.
11. K. GEMMA, T. FUJIWARA, Y. SATOH, I. USHIOKU and M. KAWAKAMI, in "Report of the Japanese Society for Heat Treatment", 39th Meeting, Kogakuin Institute of Technology, Tokyo, Japan (The Japanese Society for Heat Treatment, Tokyo, 1994) p. 67.
12. K. H. JACK, *Proc. R. Soc.* **A195** (1948) 34; (JCPDS CARD No 6-0627).
13. E. T. TURKDOGAN and S. INGATOWICE, *J. Iron Steel Inst. (Lond.)* **188** (1958) 242 (JCPDS 11–65).
14. K. H. JACK, in "Heat Treatment '73" (The Metals Society, London, 1975) p. 39.
15. E. J. MITTEMEIJER, *J. Metals* **37** (1985) 16.
16. C. WAGNER, *Z. Electrochem.* **63** (1959) 772.
17. R. A. RAPP, *Acta Metall.* **9** (1961) 730.
18. L. E. KINDLIMANN and G. S. ANSELL, *Metall. Trans.* **1** (1970) 163.
19. J. CRANK, in "The Mathematics of Diffusion" (Clarendon Press, Oxford, 1975) p. 100.
20. P. GLANSDORFF and I. PRIGOGINE, in "Thermodynamic Theory of Structure, Stability and Fluctuations" (Wiley-Interscience, London, 1974) Ch. 7.4.
21. H. HAKEN, in "Synergetics – An Introduction, Nonequilibrium Phase Transition and Self-Organization in Physics, Chemistry and Biology" (Springer, Berlin, Heidelberg, 1978) Ch. 5.4.
22. D. H. EVERETT, in "An Introduction to the Study of Chemical Thermodynamics" (Longmans Green, UK, 1959).
23. I. PROCACCIA and GITTERMANN, *Phys. Rev. Lett.* **46** (1981) 1163.
24. I. R. KRICHECSKII, Yu. V. TSEKHANSKAYA and Z. A. POLYAKOVA, *Russ. J. Phys. Chem.* **40** (1966) 715.
25. L. S. DARKEN, in "Proceedings of a Symposium for The Physical Chemistry of Metallic Solutions and Intermetallic Compounds", The National Physical Laboratory. Paper 4G (HMSO, London, 1958) p. 88.

Received 25 April
and accepted 23 November 1995